

## Pectin-based films produced by electrospraying

Victor A. Gaona-Sánchez,<sup>1</sup> Georgina Calderón-Domínguez,<sup>1</sup> Eduardo Morales-Sánchez,<sup>2</sup>  
J. Jorge Chanona-Pérez,<sup>1</sup> Israel Arzate-Vázquez,<sup>3</sup> Eduardo Terrés-Rojas<sup>4</sup>

<sup>1</sup>ENCB-Instituto Politécnico Nacional, Departamento De Ingeniería Bioquímica, Prolongación De Carpio y Plan De Ayala S/N, Casco De Santo Tomás, C.P. 11340, México, D.F., México

<sup>2</sup>CICATA-Unidad Querétaro-Instituto Politécnico Nacional, Cerro Blanco No. 141, Col. Colinas Del Cimatario, C.P. 76090, Santiago De Querétaro, Querétaro, México

<sup>3</sup>CNMN-Instituto Politécnico Nacional, Luis Enrique Erro S/N, U. Prof. Adolfo López Mateos, México, D.F. 07738, México

<sup>4</sup>Instituto Mexicano Del Petróleo (IMP), Eje Central Lázaro Cárdenas 152, San Bartolo Atepehuacan, México, D.F. 07730, México

Correspondence to: G. Calderón-Domínguez (E-mail: gcalderondominguez@gmail.com)

**ABSTRACT:** Electrospraying technique was used for the production of pectin films obtaining transparent and flexible products with thicknesses of  $23.4 \pm 3.04 \mu\text{m}$  and requiring a lower pectin solution volume ( $2.67 \times 10^{-3} \text{ mL}$ ) than casting ( $5.97 \times 10^{-3} \text{ mL}$ ) to produce films of the same area and thickness; the physical, structural, and thermal characteristics of these films were evaluated. Electrosprayed films were slightly more transparent, and with smoother surface than those obtained by casting, but with more and smaller internal pores, resulting in different film densities ( $0.7 \text{ g/cm}^3$  electrospraying,  $1.7 \text{ g/cm}^3$  casting), that could be linked to the larger water vapor permeability value obtained. These changes could be related to a physical phenomenon, seeing as the percentage of crystallinity and melting temperature remained invariable for both films. These results show that the electrospraying technique has potential in areas such as wound dressings, tissue engineering, and the release of drugs. © 2016 Wiley Periodicals, Inc. *J. Appl. Polym. Sci.* **2016**, *133*, 43779.

**KEYWORDS:** electrospinning; electrospraying; films; hydrophilic polymers

Received 17 September 2015; accepted 5 April 2016

DOI: 10.1002/app.43779

### INTRODUCTION

Nanotechnology is a promising field that involves the quantification, modeling, creation, and manipulation of materials at the nanometric scale.<sup>1–3</sup> Among nanotechnology advances, different techniques have been developed to build nanoparticles, including the electrospraying technique (electrohydrodynamic atomization). In this process, a solution of a natural or synthetic polymer is forced through a capillary tube (nozzle) where the solution acquires enough electric forces (charges) to overcome those of surface tension, resulting in a destabilization of the emerging droplet. This instability can cause the drop to transform into a series of microscopic pearls or into a stream of fluid that is deposited into a collector,<sup>4–7</sup> producing materials at nano, micro, or macroscales. Due to the repulsion of charges, the droplets are dispersed and do not merge during their flight, leading to the deposition of particles or films depending on the physical properties of the solution (viscosity, conductivity, and surface tension) and the process parameters (distance to the collector, flow rate, ambient humidity, and voltage).<sup>5,8–11</sup>

Electrospraying can be widely applied to both industrial processes and scientific instrumentations. Interest in electrospraying

has recently prompted the search and development of effective processes that enable to obtain different products for applications in several systems (e.g., medical powder production, fine metal powder production, electrostatic painting, and fuel injection, ingredient dosage in the cosmetic and food industries). However, few electrospraying researches using food grade materials have been conducted.<sup>12,13</sup>

Currently, many biopolymers such as lipids,<sup>14</sup> proteins,<sup>15</sup> and carbohydrates<sup>16–19</sup> have been studied via electrohydrodynamic atomization techniques, to produce nanofibres,<sup>18–20</sup> and wall materials for encapsulation processes,<sup>21</sup> but none of them have been reported to be used for the production of films by this technique, with the exception of zein.<sup>22</sup>

Regarding polysaccharides, different types of materials have been used for film elaboration such as cellulose,<sup>23</sup> chitosan,<sup>24</sup> starch,<sup>25</sup> and pectin,<sup>26</sup> but in all cases they were obtained by the traditional construction technologies, such as casting,<sup>27</sup> extrusion,<sup>28</sup> or spraying,<sup>29</sup> and to the best of our knowledge, there are no publications related to the production of pectin or other carbohydrates films by the electrospraying process, even though electrospraying is a well-established technology.<sup>30</sup>

On the other hand, due to the hydrocolloidal and polyelectrolytic properties of pectin such as: water retention, stability, polyfunctionality, cation exchange, and the ability to adsorb organic lipid substances, besides its biodegradable nature, flexible structural network, biocompatibility, nontoxicity, effective in bacterial inhibition, and low production cost,<sup>18,19,31,32</sup> this polysaccharide is considered a useful raw material for film applications (edible coatings, tissue engineering, wound dressings, gene transfer, and the administration and release of drugs).<sup>18,19,33,34</sup> Until today, there are not reports in the literature of films produced by electrospraying using water soluble biopolymers such as pectin, because of the special conditions required to atomize this type of solution. This scanty technological development of electrosprayed films can be related with the problems that arise during the atomization of the fluid, due to the ionization of water molecules at high voltages in an air environment that can cause corona discharges. Besides, the high values of surface tension of the biopolymers solubilized in water hinder the formation of stable jets during the electrohydrodynamic atomization.<sup>12,16–18,35</sup> As a consequence, although the electrospraying is a promising technique, many process parameters are required to be controlled, making the study to be very complex.<sup>4,13</sup> Thus, the aim of this work was to study the feasibility of generating pectin films with organic substances by the electrospraying technique, evaluating their physical and structural characteristics as well as their barrier and thermal properties, as a first step toward the development of pectin films by this technique.

## EXPERIMENTAL

### Materials

Pectin from citrus peel (P9135, Sigma-Aldrich, Mexico) with a galacturonic acid content greater than or equal to 74.0% (dried basis) was used for the elaboration of films, employing glycerol as plasticizer (G5516, Sigma-Aldrich, Mexico), Tween 20 as surfactant (P1379, Sigma-Aldrich, Mexico), and distilled water as the dilution medium.

### Film Obtention

**Pectin Solution Preparation.** A pectin solution (2% w/w) was prepared as described by Semde *et al.*<sup>36</sup> with some modifications. This solution was stirred (Corning PC 320 Hot Plate Stirrer, Tewksbury, MA) for 45 min at 550 rpm and subsequently, glycerol was added as a plasticizer at 22.2% (w/w) based on pectin and agitated for 20 more minutes. The type and level of plasticizer (glycerol) was selected based on reported casting studies.<sup>18,37</sup> Finally, Tween 20 in a ratio 1:10 w/w (Tween 20: pectin) was added into this solution as a surfactant and agitated for 30 more minutes.

The pectin solution was evaluated with respect to viscosity, conductivity, density and pH, values that were used as control quality parameters for the process.

1. Viscosity ( $\mu$ ). This parameter was determined following the methodology reported by Yuliarti *et al.*,<sup>38</sup> using a rheometer (Anton Paar Physica MCR 101, Graz, Austria) with a system of a paddle stirrer that was designed to measure viscosity in biopolymer solutions (ST24-2D/2V/2V-30). The test was con-

ducted at a constant shear rate ( $100 \text{ s}^{-1}$ ) and at room temperature ( $22 \text{ }^\circ\text{C}$ ). The viscosity was reported in Pascal-second (Pa s), and the measurements were performed in triplicate.

2. Conductivity ( $\sigma$ ). This parameter was determined following the two-point resistivity technique Calixto-Rodríguez and Sánchez-Juárez<sup>39</sup> using a multimeter (LCR HiTester, HIOKI Model 3532-50; Nagano, Japan), which also recorded the resistance ( $R$ ) values at three different frequencies (50, 100, and 1000 Hz). Equation (1) was employed for the calculation of  $\sigma$ .

$$\sigma = R * \frac{L}{A} \quad (1)$$

where  $\sigma$  ( $\text{k}\Omega^{-1} \text{ m}^{-1}$ ) is the conductivity,  $R$  ( $\text{k}\Omega$ ) is the measured resistance,  $L$  (m) is the distance between the two electrodes, and  $A$  ( $\text{m}^2$ ) is the transversal area of the cell.

3. The density and pH were evaluated following the 962.37 and 981.12 methods of the A.O.A.C. International.

**Electrospraying Method.** The electrospraying device consists of a syringe pump, a linear actuator for X-axis, a rotary drum collector, a variable high voltage power supply, and a hot air injector.

To obtain the films, the pectin solution was placed in the syringe pump (10 mL), which contains a needle made of surgical grade stainless steel and blunted by abrasion with an outer diameter of 0.8 mm (code 21G) and an inner diameter of approximately half the outer diameter (0.4 mm). The injection flow (4 mL/h) was provided by the linear actuator that pushes the plunger of the syringe. The syringe was fixed horizontally, and the needle was electrically connected to the positive high voltage power supply (0–30 kV DC, Model 30A24-P4 Brand Ultravolt, Ronkonkoma, NY). The ground electrode was connected to the rotary drum (10.16 cm length and 5.08 cm in diameter, 1/64" thickness with a two-dimensional finish, rotation speed 2.4 rpm). The injection flow was constant, and was fixed to the minimum value that assures the pectin solution is ejected, and the electric current was read and recorded through an ammeter (HandHeld Multimeter, Model MUL-600, Brand Steren, China) incorporated into the power supply. Hot air ( $150 \text{ }^\circ\text{C}$ , 51.4 L/h, Steren Hot Air Station CAU-280, China) was used to preheat the drum ( $80 \text{ }^\circ\text{C}$ ) and also to help dry the pectin film solution. Hot air was injected directly to the rotary drum, (on the opposite side to which the electrosprayed solution was injected). The hot air station was moved following the X-axis, according to the linear actuator speed (8.57 mm/min). The electrospraying process conditions were selected based on published information for electrosprayed zein solutions<sup>22</sup> and on data obtained through preliminary tests taking as selection criteria: (1) aspersion feasibility, (2) non-formation of fibers, (3) non-generation of an electric arc, and (4) homogeneity of the formed film, as no reports about obtaining pectin films by this technique were found: electric voltage ( $EV = 12.5 \pm 1$  kilovolts), distance between the injection point to the drum ( $DC = 4.5$  cm), solution injection flow ( $IF = 4.0$  mL/h), distance from the hot air station to the collector ( $DD = 6.0$  cm). Samples of approximately  $16 \times 10 \text{ cm}^2$  were obtained and all of them were immediately identified by applying small pieces of

tape in the side that had been in direct contact with the surface of the collector.

The samples for subsequent analysis were stored at room temperature inside a desiccator that contained a saturated solution of sodium bromide (NaBr) to maintain a relative humidity of 59.7%.

**Casting Method.** Films were developed in parallel by the casting method, using the same pectin concentration. The films were elaborated following the methodology as described by Semde *et al.*<sup>36</sup> with certain modifications. The pectin solution ( $7.14 \pm 0.05$  g) was poured into Teflon circular plates (7.1 cm in diameter). The solution was subjected to kiln-drying (TERLAB, MAH25D, Mexico) at 30 °C for 8 h. The temperature (30 °C) and the drying time were selected based on preliminary tests where at higher temperatures and shorter drying times, using a natural convection drying equipment, less transparent films were obtained. All of the samples for subsequent analysis were stored at room temperature as mentioned before for the electrospaying method.

#### Characterization of the Films

All the films were evaluated on physical parameters (thickness, color, transparency, water vapor permeability), structural characteristics (roughness and homogeneity) by microscopy tools [environmental scanning electron microscopy [ESEM], **atomic force microscopy** (AFM)], phase transition temperatures by differential scanning calorimeter (DSC), crystallinity percentage by X-ray diffraction (XRD) analysis, and mechanical properties (hardness and elastic modulus) by nanoindentation.

**Thickness.** As a film quality parameter, the thickness of the films was measured, using a digital micrometer (Fowler 54-860-001 Electronic IP54, China) following the methodology reported by Arzate-Vázquez *et al.*<sup>40</sup> The films were placed between the micrometer spindle and anvil, and the measurement was performed at the first sign of contact between the film and spindle. Ten measurements were performed on different positions of each film, and this analysis was performed in three independent samples (true replicates).

**Color.** This parameter was determined using the LCh parameters by means of a colorimeter (CR-400 Chroma Metre, Konica Minolta, Ramsey, NJ) considering the parameters  $L^*$  = lightness,  $a^*$  = red-green, and  $b^*$  = yellow-blue, and following the methodology reported by Calderón-Dominguez *et al.*<sup>41</sup> The measurements were performed in reflectance mode with the specular component included using illuminant D<sub>65</sub>. A total of ten measurements per film were taken, and the evaluation was performed in three independent samples (true replicates). The values of  $C^*$  = chrome (color saturation),  $h$  = hue angle (color tonality), were calculated according to eqs. (2) and (3), respectively.

$$C^* = \sqrt{(a^*)^2 + (b^*)^2}. \quad (2)$$

$$h = \arctan\left(\frac{b^*}{a^*}\right) \quad (3)$$

To determine the transparency [eq. (4)] of the films (% $T$ ) it was assumed that a fully transparent film would generate the

same luminosity values ( $L^*$ ) as those obtained from the blank calibration plate and that any difference would be the result of more opaque material ( $L^* < 100$ ).<sup>42</sup> The values obtained were analyzed with the SigmaPlot 12.0 software (Systat Software, San Jose, CA) by applying a two-way analysis of variance (ANOVA), at a significant level of  $p < 0.05$ .

$$L^* = \%T. \quad (4)$$

**ESEM.** The structure of the pectin films obtained by electrospaying and casting was examined by ESEM. The samples were directly placed on cylindrical aluminum microscope stubs using double-sided tape. The micrographs were acquired with a XL30 ESEM (Philips, Amsterdam, Holland) using an acceleration voltage of 25 kV and secondary electron detector (GSE) for the microscopic film surface evaluation and 15 kV and a secondary electron detector (BSE) for microscopic film transversal section. Samples for cross-section observations were cryofractured by immersion in liquid nitrogen.

**AFM.** Surface topography and roughness of the pectin films elaborated by electrospaying and casting, were studied by the AFM technique (diMultimode AFM microscope, Veeco, Santa Barbara, CA) with a diNANOSCOPE V controller using RTESP probes (Bruker, Camarillo, CA) with a resonance frequency of 286–362 kHz and a force constant of 20–80 N m<sup>-1</sup> in tapping mode. A 0.5 cm × 0.5 cm section was cut from each sample, attaching it to a stainless steel disc using double-side adhesive tape. Four areas of different sizes (1 × 1, 2.5 × 2.5, 5 × 5, and 10 × 10 μm<sup>2</sup>) were scanned at a speed of 1.5 Hz. The surface roughness was measured from the images using the square root of the height deviation [ $R_q$ , eq. (5)]. Also, the arithmetic mean of the height deviation absolute values [ $R_a$ , eq. (6)] was calculated using the Nano Scope Analysis 1.20 program (Veeco) and through the application of a flattening process (one degree).

$$R_q = \sqrt{\frac{\sum (Z_i)^2}{N}}. \quad (5)$$

$$R_a = \frac{1}{N} \sum_{i=1}^N |Z_i|. \quad (6)$$

where  $Z_i$  is the height deviation from the mean of the heights, and  $N$  is the number of points in the image.

**DSC.** Thermal analysis was performed in a DSC (Mettler DSC1 STAR System, Mettler Toledo, Switzerland) equipped with an oven with a FRS5 sensor. Samples of approximately  $3.0 \pm 0.1$  mg were weighed (Denver Instruments balance, model APX. 200, Bohemia, NY) inside a 40 μL aluminum sample holder, which was hermetically sealed and then perforated (a hole at the cover center). For the experiment, the heating rate was 10 °C min<sup>-1</sup> at a temperature interval of 10–400 °C with nitrogen (N<sub>2</sub>) as the purging gas at a flow rate of 50 mL min<sup>-1</sup> and with a cooling gas line at a flow rate of 2 mL min<sup>-1</sup>, which used an empty aluminum sample holder as the reference. The instrument was calibrated with an indium/zinc standard (99.98% purity, melting point of 156.6 °C and enthalpy of fusion of 28.71 J g<sup>-1</sup>). Three independent samples (true replicates) of each film were evaluated and the melting temperature ( $T_m$ ) determined as reported by Iijima *et al.*<sup>43</sup>

**Water Vapor Permeability.** The water vapor permeability (WVP) was determined using a modification of the standard gravimetric method known as the “cup method” or “test cell,” which is based on the American Society for Testing and Materials (ASTM) E 96-88 and ASTM E 96-92 methods with some variations.<sup>44,45</sup> For this test, the permeation was measured while maintaining a temperature of 30 °C and a relative humidity (RH) gradient of 100-0% through the films by placing distilled water on the permeation cell (100% RH) and anhydrous silica gel outside of the cells (0% RH). The samples were trimmed to obtain a circular sample 51.1 mm in diameter, and the samples were placed in permeation cells. The change in weight of the cell was recorded every 30 minutes in an analytical balance with a precision of 0.0001 g (DENVER instrument, Goettingen, Germany) as a function of time.

The data of the weight loss kinetics were used to calculate the permeability [eq. (7)]. The tests were performed in triplicate.

$$\text{WVP} = \frac{\text{WVTR}}{(S) \times (\%RH_1 - \%RH_2)} \times L [=] \frac{\text{g}}{\text{m Pa}} \quad (7)$$

where: WVTR = is the result obtained when dividing the value of the weight loss kinetic curve slope (g/s) by the area (m<sup>2</sup>) of the sample subjected to the test; *S* is the saturation vapor pressure in Pascals (Pa) at the test temperature; %RH<sub>1</sub> and %RH<sub>2</sub> are the relative humidity values in the test inside and outside the permeation cell, respectively, expressed as fractions; and *L* is the film thickness (m).

**XRD Analysis.** Diffraction patterns were obtained from a PANalytical XPert PRO diffractometer (Westborough MA) with Cu K $\alpha$  radiation ( $\lambda = 1.5418 \text{ \AA}$ ) (tube operating at 45 kV and 40 mA). The scanning regions were collected from 5 to 60° (2 $\theta$ ) at steps of 0.01 degrees and a step time of 100 s. The crystallinity percentage (%C) of the films was calculated from the ratio of area of all crystalline peaks to the total area with the help of software Peak Fit v4.12. It was calculated using the following eq. (8),<sup>36,46</sup>

$$\%C = \frac{\text{Crystalline area}}{\text{Total area}} \times 100. \quad (8)$$

**Mechanical Properties.** The hardness and elastic modulus were determined following the methodology reported by Escamilla-García *et al.*,<sup>42</sup> using a nanoindenter (CSM Instruments Nanoindenter, Peseux, Switzerland). The indentation was performed by applying a maximum load of 5.0 mN at a loading and unloading rate of 15 mN/min and a pause of 15 s using a Berkovich tip. The values of hardness (MPa) and the elastic modulus (GPa) were reported.

The load at break and Young's modulus were determined at room temperature using a texturometer (TA Plus, Lloyd Instrument, Ametek, England) according to the ASTM D882 standard method (ASTM 1995) and ASTM D638-01 (ASTM 2001). These parameters are directly calculated by the computer through the NEXIGENTM MT data analysis software program (Ametek, England). Films were cut into strips (longitudinal sections). The dimensions of the strips were 5 × 1.0 cm, and each one were mounted between the grips of the instrument probe. From each type of films, at least seven strips (triplicate independent) were



**Figure 1.** Pectin film obtained by electrospaying process. The small white squares of tape indicate the face of the film that was in direct contact with the surface of the collector. [Color figure can be viewed in the online issue, which is available at [wileyonlinelibrary.com](http://wileyonlinelibrary.com).]

evaluated. The grip distance and speed were 0.03 m and 0.001 m/s, respectively.

#### Statistical Analysis

The data were statistically evaluated by a two way ANOVA ( $p < 0.05$ ) using the SigmaPlot V12.0 software. The reported values are the averages and standard deviations of at least three repetitions of each sample.

## RESULTS AND DISCUSSION

### Electrospaying Process Yield

Under the operating conditions (EV = 12.5 kV; DC = 4.5 cm; IF = 4.0 mL/h; DD = 6.0 cm), it was possible to atomize the pectin solution (pH = 3.96 ± 0.11,  $\mu = 0.123 \pm 0.01 \text{ Pa s}$ ,  $\rho = 1.02 \pm 0.009 \text{ g/cm}^3$ ,  $\sigma = 115.9 \pm 4.4 \text{ k}\Omega^{-1} \text{ m}^{-1}$ ) to produce a transparent and flexible film (Figure 1), with a thicknesses of 23.4 ± 3.04  $\mu\text{m}$ , and a film density of 0.70 g/cm<sup>3</sup>, easy to handle and to remove from the barrel. Process time to obtain this film was 2.5 h. Regarding the casting process a transparent and flexible pectin film was also obtained, with a film thickness and density of 29.6 ± 2.7  $\mu\text{m}$  and 1.70 g/cm<sup>3</sup>, respectively.

As a way to compare the electrospaying and casting techniques, the process yield (*Y<sub>p</sub>*) was evaluated considering it as the volume of pectin solution (mL) fed (casting or electrospaying) to obtain a film with a surface of 1 cm<sup>2</sup> and one micron thickness [eq. (9)]:

$$Y_p = \frac{V_s}{A_f \times X_f} \quad (9)$$

where *V<sub>s</sub>* is the volume of pectin solution used to produce the films (7 mL for casting, 10 mL for electrospaying), *A<sub>f</sub>* is the film area (39.59 cm<sup>2</sup> casting, 160 cm<sup>2</sup> electrospaying), and *X<sub>f</sub>* is the film thickness (29.6 ± 2.7  $\mu\text{m}$  via casting, 23.4 ± 3.04  $\mu\text{m}$  via electrospaying).

Based on these calculations, it was found that 2.67 × 10<sup>-3</sup> mL of pectin solution are required for the electrospaying method while 5.97 × 10<sup>-3</sup> mL for casting. These figures show that the electrospaying process required a lower pectin solution volume than casting to produce films of the same area and thickness. This could be related with smaller processing costs, but an energy cost balance would be necessary to have a more real

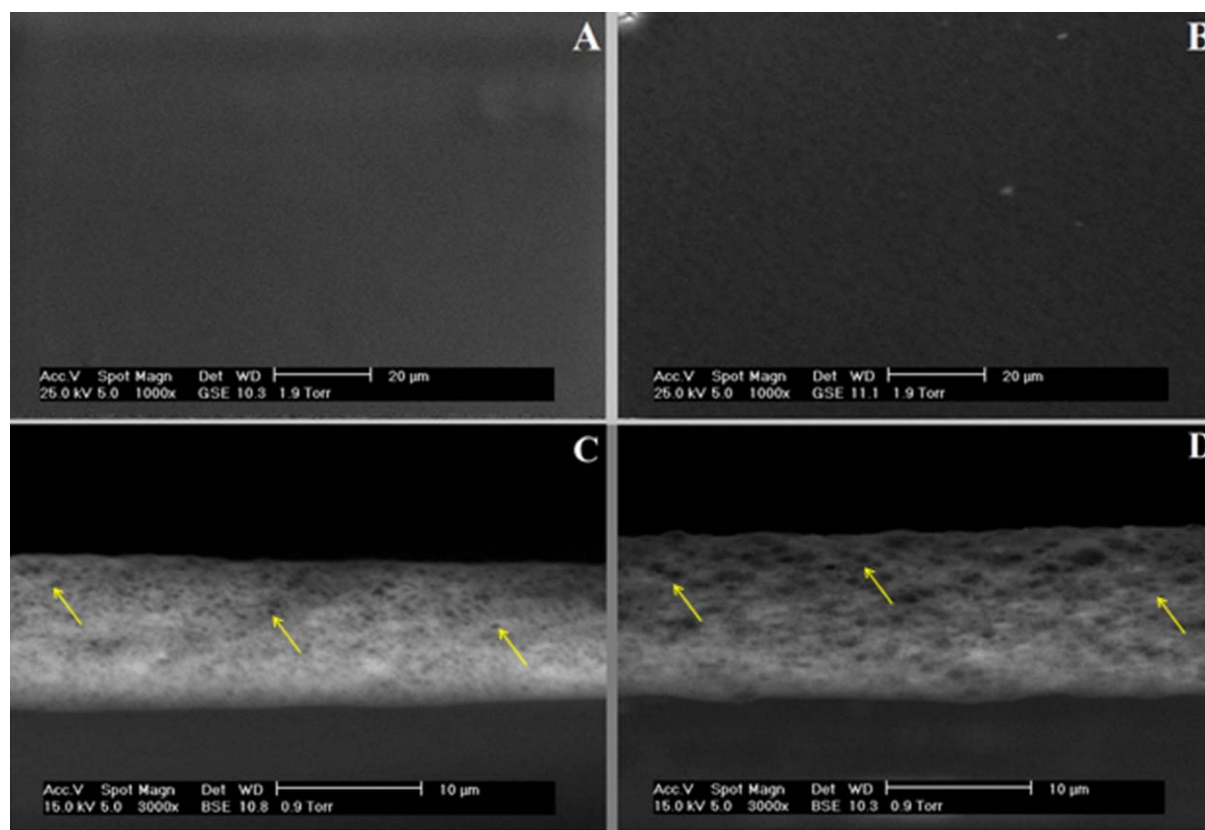


**Figure 2.** ESEM images of surface ( $\times 1000$ ) and transversal section ( $\times 3000$ ) of pectin films produced by electrospaying (A–C) and casting (B–D) techniques. Arrows in the micrographs show the presence of pores in the films. [Color figure can be viewed in the online issue, which is available at [wileyonlinelibrary.com](http://wileyonlinelibrary.com).]

view of the advantages of the electrospaying process, which was not considered in the objectives of this study.

### Color

Color attributes are important factors in foods products because they directly influence its acceptability to the consumer. Accordingly, biopolymer-based films and coatings must be as close to colorless as possible or present a coloration and transparency that does not affect product acceptability.<sup>47</sup> The values obtained for the pectin films prepared by electrospaying ( $\%T = 96.65 \pm 0.16$ ,  $C^* = 3.7 \pm 0.20$ ,  $h^* = 91.1 \pm 0.47$ ) were statistically different ( $p < 0.05$ ) to those obtained by casting ( $\%T = 95.73 \pm 0.52$ ;  $C^* = 5.8 \pm 0.54$ ,  $h^* = 91.8 \pm 0.12$ ), with the electrospayed product being slightly more transparent ( $\%T$ ). However, both films tended to be colorless, as color saturation (chroma) and tonality (hue angle) tended to be low. This effect may be due to the differences in thickness, as well as to the preparation method.<sup>22</sup> In this regard, Galus and Lenar (2013) reported less transparent ( $L = \%T = 89.3$ ), but with similar values for  $C^*$  (5.8) for pectin films produced by the casting method, as compared to those obtained in this work, but different to the ones produced by the electrospaying technique.

### ESEM

To obtain a better view of the film homogeneity, surface and transversal section micrographs were acquired (Figure 2). The results of the film surface morphology showed that the samples

produced by electrospaying [Figure 2(A)] presented a more homogenous surface in comparison to those produced by casting [Figure 2(B)], which displayed small holes. Regarding the film cross section micrographs of electrospayed sample [Figure 2(C)], apparently the inner structure of the film has more and smaller pores than those observed in the sample obtained by casting [Figure 2(D)], resulting in different film densities ( $0.7 \text{ g/cm}^3$  electrospaying,  $1.7 \text{ g/cm}^3$  casting). This open structure can be related to the way the droplet impacts and interacts with the substrate. In this regard, Eslamian<sup>48</sup> cited that when spraying-on to produce films, the droplet impact on substrate is related to a nucleate boiling, resulting in the formation of cavities. Regarding the more homogeneous surface of the electrospayed films, this could be due to the filling of pores by the droplets that impact on the surface over a previously deposited layer<sup>6</sup> or to a faster drying, solute adhesion and bonding on the surface of the film.

On the other hand, the presence of pores in pectin films produced by casting has been previously reported by Murillo-Martínez *et al.*,<sup>49</sup> Jo *et al.*,<sup>50</sup> and Kang *et al.*,<sup>51</sup> and this phenomenon has been attributed to the differential surface tension during solution drying.<sup>31</sup>

With respect to electrospaying, it has been reported that a more homogenous zein film can be produced by this technique.<sup>18</sup> No published micrographs were found for pectin films produced by electrospaying.

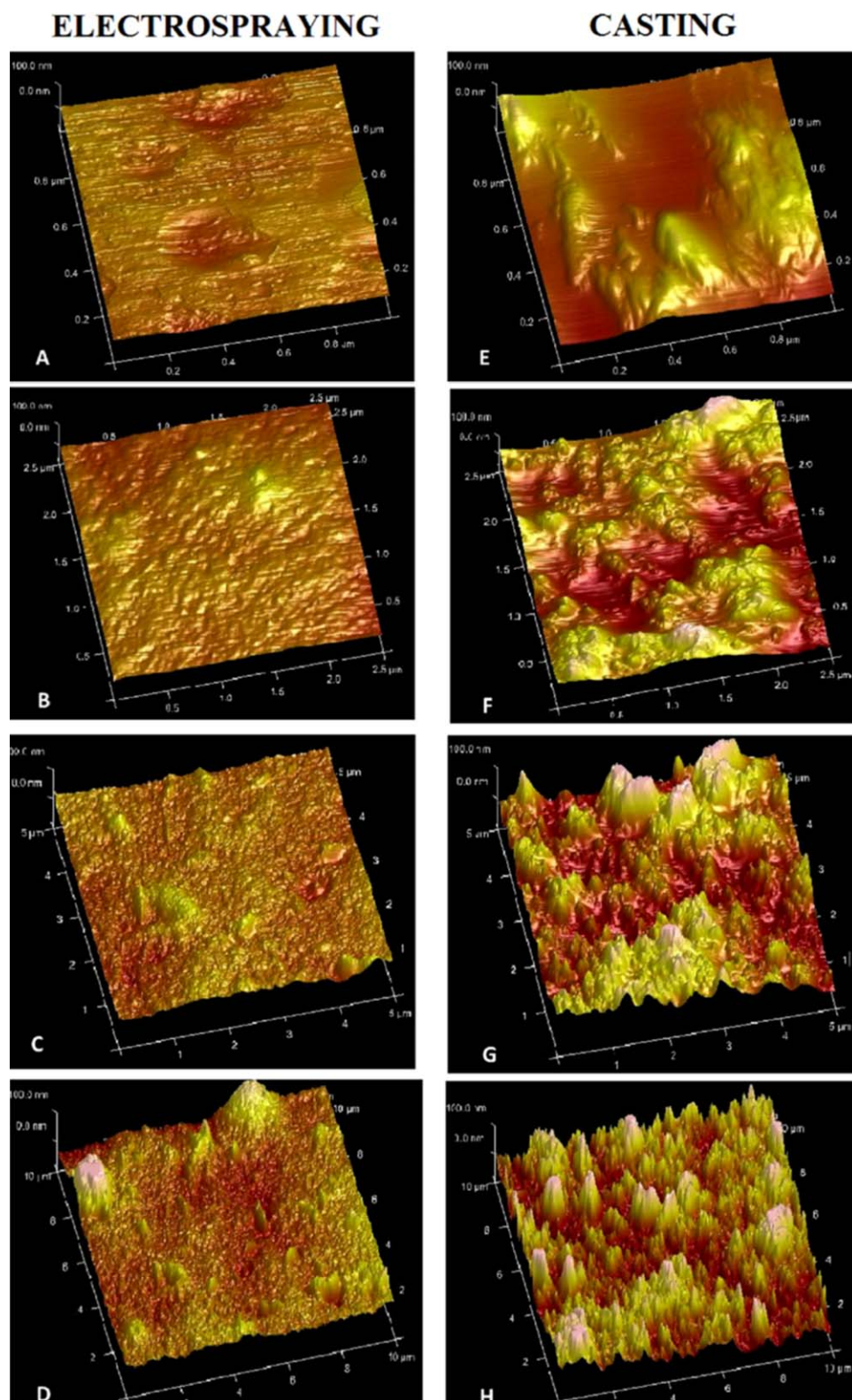


**Figure 3.** AFM height 3D images of pectin films prepared by electrospaying (A–D) and casting (E–H) at different scanning areas (1.0, 2.5, 5.0, and 10.0  $\mu\text{m}^2$ ). [Color figure can be viewed in the online issue, which is available at [wileyonlinelibrary.com](http://wileyonlinelibrary.com).]

### AFM

For pectin films prepared by electrospaying [Figure 3(A–D)], the AFM micrographs show the absence of imperfections, such

as small holes, pores and fractures, thus confirming a continuous surface, as observed by ESEM, [Figure 2(A)]. When comparing the surfaces produced via casting, a less smooth surface

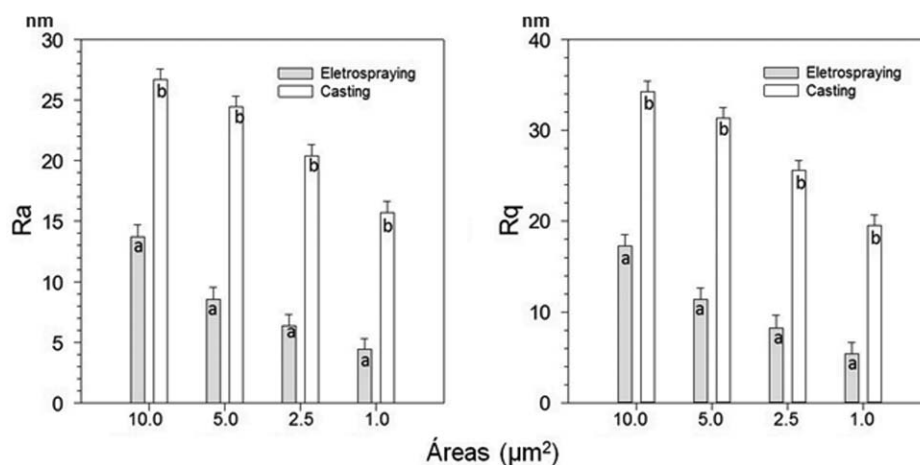


**Figure 4.** Roughness mean values ( $R_a$  and  $R_q$ ) of pectin films prepared by electro spraying or casting at four different scanning areas (10.0, 5.0, 2.5, and 1.0  $\mu\text{m}^2$ ). Different letters by scanning area indicate a significant difference between methods ( $p < 0.05$ ).

was observed [Figure 3(E–H)]. In this regard, it has been reported that the electro spraying technique used in the preparation of zein films tends to produce smoother surfaces while the thickness of the film does not have a significant effect on this parameter.<sup>22</sup>

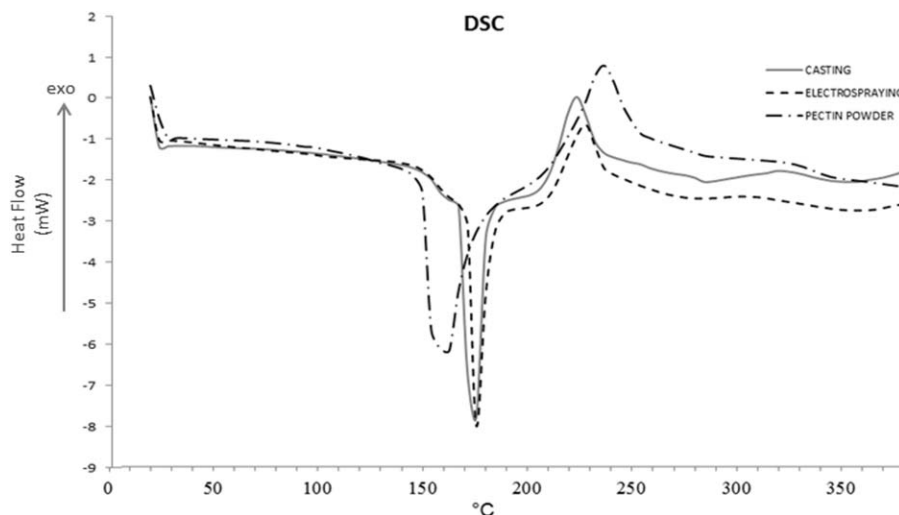
Based on the above findings, statistical analysis of the  $R_q$  and  $R_a$  values of the films prepared by both methods was performed, showing  $R_q$  values from  $17.22 \pm 1.9$  to  $5.36 \pm 0.92$  and  $R_a$  values from  $13.66 \pm 2.22$  to  $4.41 \pm 0.85$ , depending on the area scanned (Figure 4). In all cases, the roughness values showed a tendency to be significantly lower ( $p < 0.05$ ) as a result of the area scanned and the preparation method for films (electro spraying and casting, Figure 4).

This finding may be because electrohydrodynamic atomization is a process in which fine and semi-solid droplets of a material impinge on a substrate, then spread to form a product where the droplets that impact the surface over the previously deposited layer could penetrate into sites where pores may be present, resulting in a smoother surface.

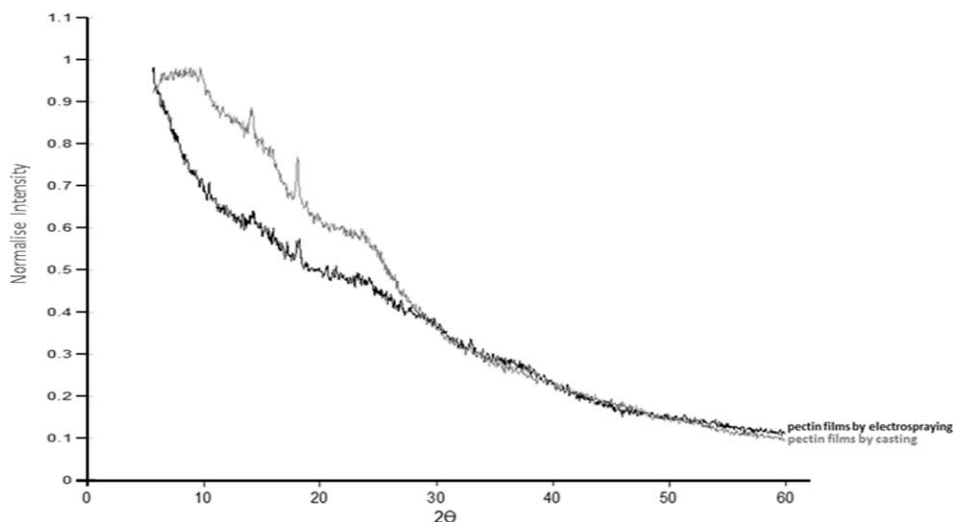
## DSC

Figure 5 shows the thermograms corresponding to pectin powder and to pectin films produced via electro spraying as well as casting. As shown in Figure 5, there is a melting temperature ( $T_m$ ) value of  $175.61 \pm 0.04$  °C for the films produced by electro spraying, which has no significant difference ( $p > 0.05$ ) with respect to the value of those produced by casting ( $175.69 \pm 0.16$  °C). However, both  $T_m$  are higher than that of pectin powder ( $162.71 \pm 0.07$  °C). This difference may be due to intramolecular interactions between pectin, glycerol and/or Tween 20.<sup>52</sup>

In the same thermograms, it was possible to observe an exothermic peak at  $227.96 \pm 0.01$ ,  $223.67 \pm 0.04$ , and  $236.71 \pm 0.02$  for films prepared by electro spraying, casting, and pectin powder, respectively. In these regard, Einhorn-Stoll and Kunzek,<sup>53</sup> reported that pectin powder undergoes a thermal degradation, observed as a DSC exothermic peak, that starts at 200 °C and ends at about 240–280 °C, depending on the molecular parameters, the degree of esterification, and the physical state. Soares



**Figure 5.** Thermograms of pectin powder, and pectin films prepared by electro spraying and casting methods. Casting: solid line; Electro spraying: dash line; Pectin powder: dash-dot line.



**Figure 6.** X-ray diffractogram of pectin films prepared by electrospinning and casting. Intensity data was normalized for both samples, considering their highest value.

*et al.*<sup>54</sup> attributed these values to the pectin decomposition by an oxidation reaction. The results obtained in our work are similar to those reported by Einhorn-Stoll *et al.*<sup>55</sup> and Einhorn-Stoll and Kunzek.<sup>53</sup> Based on the above finding, it can be noticed that under the conditions of this study, the preparation method does not modify the melting capacity of the pectin film ( $T_m$ ), but it slightly does at the DSC exothermic point.

### WVP

Regarding WVP of the films, the values obtained were  $5.61 \pm 0.78 \times 10^{-09}$  (g)/(s m Pa) for those elaborated by electrospinning and  $3.87 \pm 0.3 \times 10^{-09}$  (g)/(s m Pa) for the films prepared by casting; these values were significantly different ( $p < 0.05$ ), which means that the method influences the film formation, being these values within the order of magnitude of the information reported by Pérez *et al.*<sup>56</sup> for films of high-methoxyl pectin with methylcellulose [ $1.2\text{--}1.5 \times 10^{-09}$  (g)/(s m Pa)]. The WVP values obtained from the pectin films produced by electrospinning show that this technique, does not alter the order of magnitude of the permeability values of the produced films, but tends to form more porous structures, allowing the pass of gases or water vapor, which could be useful, not for barrier purposes but for tissue engineering, wound dressings, and the administration and release of drugs.<sup>33,34</sup>

### XRD Analysis

With respect to the XRD patterns (Figure 6), both patterns (pectin films by electrospinning and pectin films by casting) presented two peaks, one at 14 and the other at 18 degrees  $2\theta$  approximately. This analysis indicates no significant change ( $p > 0.05$ ) in the crystallinity of the films, nor between the methods of processing, showing an amorphous structure in both of them. The XRD patterns yielded a %C of  $6.8 \pm 0.25$  and  $6.7 \pm 0.30$  for pectin films prepared by electrospinning and casting, respectively.

### Mechanical Properties

Regarding mechanical properties, electrospayed films showed values, obtained by nanoindentation, of  $15.2 \pm 3.56$  MPa and  $0.067 \pm 0.011$  GPa for hardness and elastic modulus, respectively, while those obtained by casting exhibited values of  $82.6 \pm 13.0$  MPa for hardness and  $0.74 \pm 0.11$  GPa for elastic modulus. This information indicates that the electrospayed film is more flexible and with less hardness than the one prepared by casting. These results could be due to the difference in thickness between films, as well as to the differences in their structures, mainly the porosity, as pointed out by Chen *et al.*<sup>57</sup> who refer that the decrease in the values of hardness and elastic modulus is related to an increase in the porosity of the samples, due to that the hardness is more influenced by a structure with larger densification, which is to be expected, since the hardness (plastic deformation) of these materials is controlled by crushing rather than the more usual plastic deformation (viscous flow or dislocation motion) seen in other materials.

The results corresponding to the load at break and Young's modulus analysis for electrospayed films, as obtained with the TA plus texture meter, were  $4.66 \pm 0.79$  N and  $882.25 \pm 162.78$  MPa, respectively, while both parameters for films obtained by casting, with the same equipment, were larger (load at break =  $12.20 \pm 2.55$  N and Young's modulus =  $1382.14 \pm 237.76$  MPa) indicating that the electrospayed films were more flexible than those by casting. It is important to mention that even these results follow the same path than those obtained using the nanoindenter equipment, is not possible to compare results among them, as the type of probe, the size of the sample, and the force applied are different. Nanoindentation is based on a penetration evaluation (Berkovich tip), while the texture meter results are based on tensile forces (extension) giving as a result values in a very different order of magnitude.

### CONCLUSIONS

The present work reports the production of films based on polysaccharides such as pectin by electrospinning, using water as



solvent and non-toxic and biocompatible additives, resulting in films with different physical characteristics as compared to those obtained by casting, mainly in their porosity, mechanical (hardness and elastic modulus) and barrier properties (WVP). These differences seem to be more related to a physical phenomenon than to chemical interactions. The results of this study demonstrate that the electrospaying technique can be used to produce films with some properties that could be of interest for the medical and pharmaceutical areas, using lower amounts of raw materials as compared to casting. However, more studies in this area are needed.

## ACKNOWLEDGMENTS

V.A. Gaona-Sánchez wishes to express its gratitude to CONACYT and PIFI-IPN for the scholarships provided. This research was funded through projects 20151383, 20140625, 20140827 from National Polytechnic Institute (IPN-Mexico) and 1668, 133162 from CONACYT. The authors also wish to thank the Mexican Petroleum Institute (IMP) and the Centre for Nanoscience and Micro and Nanotechnology (CNMN-IPN) for the analysis carried out and the technical assistance.

## REFERENCES

- Jahangiri, A.; Davaran, S.; Fayyazi, B.; Tanhaei, A.; Payab, S.; Adibkia, K. *Colloids Surf. B* **2014**, *123*, 219.
- Anu Bhushani, J.; Anandharamakrishnan, C. *Trends Food Sci. Technol.* **2014**, *38*, 21.
- Gunn, J.; Zhang, M. *Trends Biotechnol.* **2010**, *28*, 189.
- Stijnman, A. C.; Bodnar, I.; Hans Tromp, R. *Food Hydrocolloids* **2011**, *25*, 1393.
- Bock, N.; Dargaville, T. R.; Woodruff, M. A. *Prog. Polym. Sci.* **2012**, *37*, 1510.
- Jaworek, A. T. S. A.; Sobczyk, A. T. *J. Electrostat.* **2008**, *66*, 197.
- Hartman, R. P. A.; Brunner, D. J.; Camelot, D. M. A.; Marijnissen, J. C. M.; Scarlett, B. *J. Aerosol Sci.* **2000**, *31*, 65.
- Aceituno-Medina, M.; Mendoza, S.; Lagaron, J. M.; López-Rubio, A. *Food Res. Int.* **2013**, *54*, 667.
- Chakraborty, S.; Liao, I.; Adler, A.; Leong, K. W. *Adv. Drug Delivery Rev.* **2009**, *61*, 1043.
- Okutan, N.; Terzi, P.; Altay, F. *Food Hydrocolloids* **2014**, *39*, 19.
- Brandenberger, H.; Nüssli, D.; Piech, V.; Widmer, F. *J. Electrostat.* **1999**, *45*, 227.
- Zhang, X.; Kobayashi, I.; Uemura, K.; Nakajima, M. *Colloids Surf. A: Physicochem. Eng. Asp.* **2013**, *436*, 937.
- Bock, N.; Woodruff, M. A.; Huttmacher, D. W.; Dargaville, T. R. *Polymers* **2011**, *3*, 131.
- Eltayeb, M.; Bakhshi, P. K.; Stride, E.; Edirisinghe, M. *Food Res. Int.* **2013**, *53*, 88.
- Kayaci, F.; Uyar, T. *Carbohydr. Polym.* **2012**, *90*, 558.
- Pérez-Masiá, R.; Lagaron, J. M.; López-Rubio, A. *Carbohydr. Polym.* **2014**, *101*, 249.
- Santos, C.; Silva, C. J.; Büttel, Z.; Guimarães, R.; Pereira, S. B.; Tamagnini, P.; Zille, A. *Carbohydr. Polym.* **2014**, *99*, 584.
- Xin, S.; Li, X.; Ma, Z.; Lei, Z.; Zhao, J.; Pan, S.; Zhou, X.; Deng, H. *Carbohydr. Polym.* **2013**, *92*, 1880.
- Zhang, T.; Zhou, P.; Zhan, Y.; Shi, X.; Lin, J.; Du, Y.; Li, Y.; Deng, H. *Carbohydr. Polym.* **2015**, *117*, 687.
- Torres-Giner, S.; Gimenez, E.; Lagarón, J. M. *Food Hydrocolloids* **2008**, *22*, 601.
- López-Rubio, A.; Sanchez, E.; Sanz, Y.; Lagaron, J. M. *Bio-macromolecules* **2009**, *10*, 2823.
- Gaona-Sánchez, V. A.; Calderón-Domínguez, G.; Morales-Sánchez, E.; Chanona-Pérez, J. J.; Velázquez-de la Cruz, G.; Méndez-Méndez, J. V.; Terrés-Rojas, E.; Farrera-Rebollo, R. R. *Food Hydrocolloids* **2015**, *49*, 1.
- Ayranci, E.; Tunc, S. *Food Chem.* **2001**, *72*, 231.
- Elsabee, M. Z.; Abdou, E. S.; Nagy, K. S.; Eweis, M. *Carbohydr. Polym.* **2008**, *71*, 187.
- Bertuzzi, M. A.; Vidaurre, E. C.; Armada, M.; Gottifredi, J. C. *J. Food Eng.* **2007**, *80*, 972.
- da Silva, M. A.; Bierhalz, A. C. K.; Kieckbusch, T. G. *Carbohydr. Polym.* **2009**, *77*, 736.
- Galus, S.; Lenart, A. *J. Food Eng.* **2013**, *115*, 459.
- Fishman, M. L.; Coffin, D. R.; Onwulata, C. I.; Willett, J. L. *Carbohydr. Polym.* **2006**, *65*, 421.
- Jindal, M.; Kumar, V.; Rana, V.; Tiwary, A. K. *Int. J. Biol. Macromol.* **2013**, *52*, 77.
- Xie, J.; Jiang, J.; Davoodi, P.; Srinivasan, M. P.; Wang, C. H. *Chem. Eng. Sci.* **2015**, *125*, 32.
- Espitia, P. J. P.; Du, W. X.; Avena-Bustillos, R. D. J.; Soares, N. D. F. F.; McHugh, T. H. *Food Hydrocolloids* **2014**, *35*, 287.
- Baeva, M.; Panchev, I. *Food Chem.* **2005**, *92*, 343.
- Ninan, N.; Muthiah, M.; Park, I. K.; Elain, A.; Thomas, S.; Grohens, Y. *Carbohydr. Polym.* **2013**, *98*, 877. 2013,
- Kaur, A.; Kaur, G. *Saudi Pharm. J.* **2012**, *20*, 21.
- Rockwell, P. L.; Kiechel, M. A.; Atchison, J. S.; Toth, L. J.; Schauer, C. L. *Carbohydr. Polym.* **2014**, *107*, 110.
- Semde, R.; Amighi, K.; Pierre, D.; Devleeschouwer, M. J.; Moes, A. J. *Int. J. Pharm.* **1998**, *174*, 233.
- Galicia-García, T.; Martínez-Bustos, F.; Jiménez-Arevalo, O.; Martínez, A. B.; Ibarra-Gómez, R.; Gaytán-Martínez, M.; Mendoza-Duarte, M. *Carbohydr. Polym.* **2011**, *83*, 354.
- Yuliarti, O.; Matia-Merino, L.; Goh, K. K.; Mawson, J.; Williams, M. A.; Brennan, C. *Food Chem.* **2015**, *166*, 479.
- Calixto-Rodríguez, M.; Sánchez-Juárez, A. *Superficies Vacío* **2007**, *20*, 34.
- Arzate-Vázquez, I.; Chanona-Pérez, J. J.; Calderón-Domínguez, G.; Terres-Rojas, E.; Garibay-Febles, V.; Martínez-Rivas, A.; Gutiérrez-López, G. F. *Carbohydr. Polym.* **2012**, *87*, 289.
- Calderón-Domínguez, G.; Vera-Domínguez, M.; Farrera-Rebollo, R.; Arana-Erasquin, R.; Mora-Escobedo, R. *Int. J. Food Prop.* **2004**, *7*, 165.
- Escamilla-García, M.; Calderón-Domínguez, G.; Chanona-Pérez, J. J.; Farrera-Rebollo, R. R.; Andraca-Adame, J. A.;

- Arzate-Vázquez, I.; Mendez-Mendez, J. V.; Moreno-Ruiz, L. A. *Int. J. Biol. Macromol.* **2013**, *61*, 196.
43. Iijima, M.; Nakamura, K.; Hatakeyama, T.; Hatakeyama, H. *Carbohydr. Polym.* **2000**, *41*, 101.
44. McHugh, T. H.; Avena-Bustillos, R.; Krochta, J. M. *J. Food Sci.* **1993**, *58*, 899.
45. Mali, S.; Grossmann, M. V. E.; García, M. A.; Martino, M. N.; Zaritzky, N. E. *J. Food Eng.* **2006**, *75*, 453.
46. Yuan, L.; Wan, J.; Ma, Y.; Wang, Y.; Huang, M.; Chen, Y. *BioResources* **2012**, *8*, 717.
47. Rhim, J. W.; Gennadios, A.; Weller, C. L.; Hanna, M. A. *Ind. Crops Prod.* **2002**, *15*, 199.
48. Eslamian, M. *Coatings* **2014**, *4*, 60.
49. Murillo-Martínez, M. M.; Pedroza-Islas, R.; Lobato-Calleros, C.; Martínez-Ferez, A.; Vernon-Carter, E. J. *Food Hydrocolloids* **2011**, *25*, 577.
50. Jo, C.; Kang, H.; Lee, N. Y.; Kwon, J. H.; Byun, M. W. *Radiat. Phys. Chem.* **2005**, *72*, 745.
51. Kang, H. J.; Jo, C.; Lee, N. Y.; Kwon, J. H.; Byun, M. W. *Carbohydr. Polym.* **2005**, *60*, 547.
52. Mishra, R. K.; Datt, M.; Banthia, A. K. *AAPS PharmSciTech* **2008**, *9*, 395.
53. Einhorn-Stoll, U.; Kunzek, H. *Food Hydrocolloids* **2009**, *23*, 40.
54. Soares, G. A.; de Castro, A. D.; Cury, B. S.; Evangelista, R. C. *Carbohydr. Polym.* **2013**, *91*, 135.
55. Einhorn-Stoll, U.; Kunzek, H.; Dongowski, G. *Food Hydrocolloids* **2007**, *21*, 1101.
56. Pérez, C. D.; De'Nobili, M. D.; Rizzo, S. A.; Gerschenson, L. N.; Descalzo, A. M.; Rojas, A. M. *J. Food Eng.* **2013**, *116*, 162.
57. Chen, Z.; Wang, X.; Bhakhri, V.; Giuliani, F.; Atkinson, A. *Acta Mater.* **2013**, *61*, 5720.